

Hadronic emission in middle-aged SNRs

ANDREA GIULIANI¹, MARTINA CARDILLO², MARCO TAVANI^{1,4},

¹ INAF / IASF Milano, via E. Bassini 15, 20133 Milano, Italy

² Dipartimento di Fisica, Universit degli Studi di Roma "Tor Vergata" via della Ricerca Scientifica 1, 00133 Roma, Italy

³ INAF-IAPSA, via Del Fosso del Cavaliere 100, 00133 Roma, Italy

giuliani@iasf-milano.inaf.it

Abstract: Recent gamma-rays observations of Supernova Remnants revealed the existence of a class of objects characterized by an age older than some thousands of years, interacting with massive molecular clouds and with a soft spectral energy distribution peaked at some hundreds of MeV. This class includes the well known SNRs W44, IC 443, W28, W51C and others. Here we present the AGILE observations of this class of SNRs in the band 50 MeV - 10 GeV. The observations in this range (especially in the lowest part, 50-100 MeV) are crucial in constraining the emission models of these objects and can be used to study the diffusion of particles in the ISM around the source. Probably the most relevant object in this class is SNR W44, for which, combining gamma-rays and radio observations, we demonstrated that lepton-dominated models fail to explain simultaneously the well-constrained multiwavelength spectrum, leading to the first unambiguous evidence of gamma-rays emission from neutral-pions decay in a SNR..

Keywords: icrc2013, Gamma Astronomy, Supernova Remnants.

1 Two classes of SNRs

Although the first clear gamma-rays identifications of SNRs are quite recent, the number of these objects grew rapidly in recent years due to observations obtained with both space (AGILE and Fermi) and ground-based (HESS, MAGIC, VERITAS) telescopes.

From a phenomenological point of view gamma-rays SNRs can be divided into two classes:

- *Class 1* objects are young ($10^2 - 10^3$ yrs) shell-like SNRs, expanding in a relatively low density medium. The morphology shown in gamma rays is usually very nicely correlated with the radio or X-rays emission from the shell (Examples : Cas A, Tycho SNR, RX J1713.7-3946 ...).
- *Class 2* objects are older ($10^3 - 10^4$ yrs) mixed-morphology SNRs, interacting with giant molecular clouds. Their gamma-rays morphology correlates with the molecular clouds associated to the SNR (Examples : W28, W44, IC 443 ...).

Figure 1 shows the gamma-rays luminosity ($E > 100$ MeV, from [15]) as a function of age for some objects of the two classes (ages and distances were taken by literature, see [13] and reference therein). The *Class 2* objects are characterized by an higher luminosity ($\sim 10^{34}$ erg / sec cm^2 for *Class 1* and $\sim 10^{36}$ erg / sec cm^2 for *Class 2*), according with the higher density of the medium in which they are expanding.

As shown in the following *Class 2* SNRs have most of their emission in the energy range where the AGILE/GRID instrument is more sensitive, namely for $E < 1$ GeV. Therefore this class of SNRs is the best suited for investigation with AGILE.

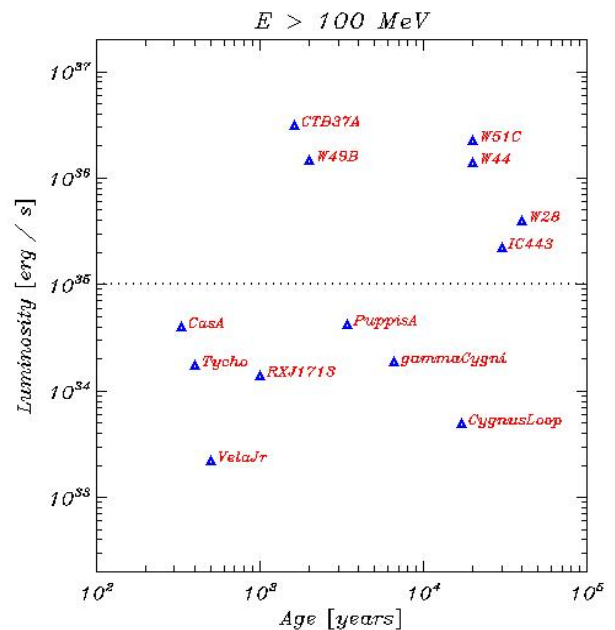


Figure 1: Gamma-rays luminosity as a function of age for some *Class 1* and *Class 2* objects.

2 The SNR W44

W44 is a middle-aged SNR (about 20000 years) expanding in a dense and very inhomogeneous medium [20]. There is evidence of interaction with the surrounding molecular clouds [17], [14]. This object is source of intense non-thermal emission in both radio band (which has been measured over the frequency range 10 MHz - 10 GHz) and gamma-rays band (from 50 MeV to 50 GeV). It is extended approximately 0.5 degrees corresponding to about 30 pc if a distance of 3 kpc is assumed. For all these features the

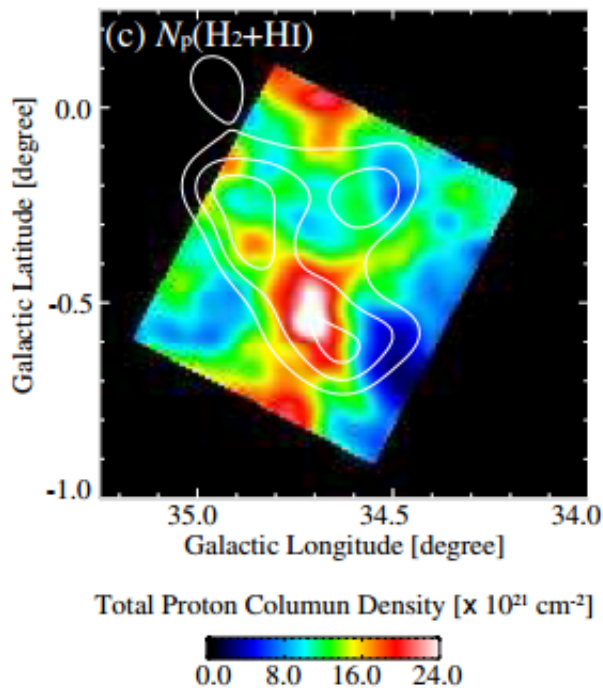


Figure 2: Total proton column density (molecular and neutral hydrogen) towards SNR W44. Adapted from [20]

supernova remnants W44 is an ideal laboratory for understanding the mechanisms of the gamma-rays emission in SNRs

The radio spectrum of W44 [8] is well represented by power-law with a spectral index of -0.37 ± 0.02 over a frequency range spanning more than three orders of magnitude. If interpreted as synchrotron emission from relativistic electrons, it corresponds to a distribution of particles with slope -1.74 in the energy range 300 MeV - 10 GeV if a magnetic field of $10 \mu\text{G}$ is assumed, or 100 MeV - 3 GeV for a magnetic field of $100 \mu\text{G}$.

2.1 The gamma-rays spectrum of W44

The gamma-rays detectors on board of Fermi and AGILE were able to measure the spectrum of W44 in the energy range 50 MeV - 50 GeV. These observations allowed to characterize the gamma-rays spectrum of W44 with an unprecedented precision. As shown in figure 2 this spectrum is characterized by a wide bump at energies of about 700-800 MeV. This spectral shape leads to remarkable insights on the population of gamma-emitting particles.

1. A single population of electrons cannot fit simultaneously the Gamma-rays and radio spectra. While gamma-rays emission from neutral pion decay can fit very nicely the spectrum. This was the first direct evidence of accelerated protons in a supernova remnant.
2. The gamma-rays spectrum is very soft for energies greater than ~ 1 GeV. This in turn implies that the protons distributions must be very hard (an index of ~ 3.5) for energies greater than few GeV up to 50 GeV.

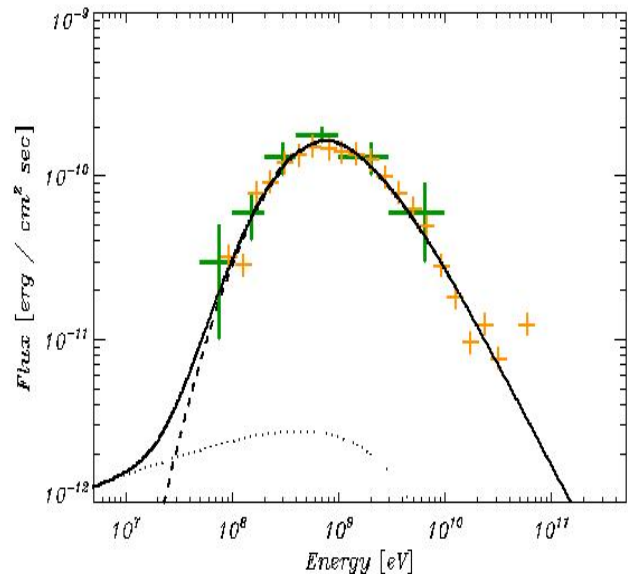


Figure 3: Gamma-rays spectrum of W44 as seen by AGILE (green data [11]) and Fermi (yellow data [3]).

3. A simple power-law overestimate the flux in the low energy part of the spectrum. This implies that the distribution of protons is strongly suppressed below few GeV.

Soft spectral index and suppression of the low energy part of the spectrum seem to be common in the emission of *Class 2* objects (it have been observed also for W28 [12], IC 443 [3], and W51C [7]).

The study of the system given by SNR W28 and their associated molecular clouds showed that diffusion of accelerated protons in the medium around this SNR can explain both the soft index and the low-energy cutoff. This suggests that diffusion of cosmic rays around *Class 2* objects is a crucial key to understand the gamma-ray emission from these systems.

3 SNR W28

W28 is a mixed morphology SNR with an age of more than 35 000 years located at a distance of about 1.9 kpc. A system of massive molecular clouds is associated to the SNR as revealed by the CO ($J=0 \rightarrow 1$) observation carried by the NANTEN telescope [9]. Two main peaks in the molecular hydrogen distribution can be seen at R.A., dec = 270.4, -23.4 (cloud N) and at R.A., dec = 270.2, -24.1 (cloud S, see fig. 4)

The molecular clouds distribution correlates nicely with the gamma rays observations in both the TeV energy band [4] and in the $E > 400$ MeV energy band observed by AGILE. However the ratio between the TeV and the multi-MeV emission is significantly different for the cloud N and the cloud S. In figure 5 the gamma-ray spectra for the two clouds are shown.

The interpretative scenario proposed in [12] assumes that the N cloud is closer to the CR acceleration site than the S cloud. If protons diffuse in the interstellar medium with a diffusion coefficient given by :

$$D(E) = D_0 E^{0.5}$$

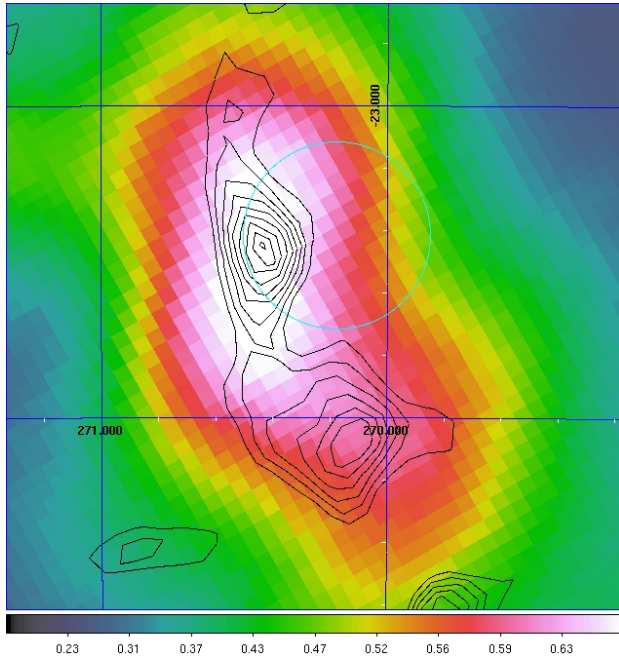


Figure 4: AGILE counts map for the W28. The blue circles indicate the location of the supernova remnant W28, the black contours show the CO intensity emission

the resulting proton energy spectrum is suppressed below a threshold energy :

$$E_t \sim R^4 t^{-2}$$

where R is the distance from the acceleration site and t the age of the SNR.

Assuming that CR are accelerated in a spherical region (indicated by the blue circle in figure 4) we evaluated the tridimensional distribution of cosmic rays $N(r,E,t)$ around the SNR as a function of the particle energy and SNR age solving the diffusion equation :

$$\frac{dN(r,E,t)}{dt} = D(E) \nabla^2 N + \frac{\partial}{\partial E} [b(E)N] + Q(E)$$

where $b(E)$ represents the energy losses, and assuming that the cosmic rays were injected impulsively with a spectrum :

$$Q(E) \sim E^{-2.2}$$

Black contours in figure 4 shows the distribution of targets (molecular hydrogen) as derived by the observations of the NANTEN telescope. Figure 5 shows the gamma-rays spectra produced by protons (through neutral pion decay) interacting with the cloud N and S assuming respectively $R = 9$ and 4 pc. This scenario can explain also the different morphology of the gamma-rays emission seen in the TeV and GeV energies ranges.

References

- [1] Abdo, A. A., Ackermann, M., Ajello, M., et al. 2010, *Science*, 327, 1103
- [2] Acciari, V. A., Aliu, E., Arlen, T., et al. 2009, *ApJ Lett.*, 698, L133
- [3] Ackermann, M., Ajello, M., Allafort, A., et al. 2013, *Science*, 339, 807

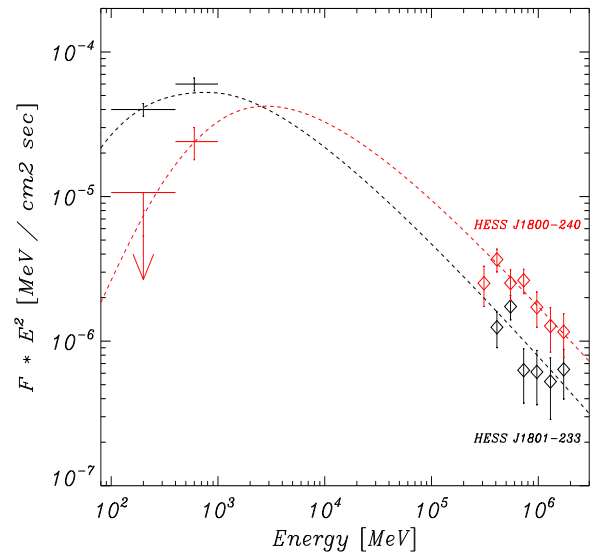


Figure 5: Combined AGILE and HESS gamma-ray photon spectra for cloud N (black) and cloud S (red). The curves represent the gamma-ray spectra estimated (according to the model presented in the text) for the two clouds.

- [4] Aharonian, F., Akhperjanian, A. G., Bazer-Bachi, A. R., et al. 2008,
- [5] Aharonian. 2006, *Astron. Astrophys.*, 449, 223
- [6] Albert, J., Aliu, E., Anderhub, H., et al. 2007, *ApJ Lett.*, 664, L87
- [7] Aleksić, J., Alvarez, E. A., Antonelli, L. A., et al. 2012, *A&A*, 541, A13
- [8] Castelletti, G., Dubner, G., Brogan, C., & Kassim, N. E. 2007, *Astron. Astrophys.*, 471, 537
- [9] Fukui, Y. 2008, in *American Institute of Physics Conference Series*, Vol. 1085, American Institute of Physics Conference Series, ed. F. A. Aharonian, W. Hofmann, & F. Rieger, 104–111
- [10] Gabici, S., Aharonian, F. A., & Casanova, S. 2009, *MNRAS*, 396, 1629
- [11] Giuliani, A., Cardillo, M., Tavani, M., et al. 2011, *ApJ*, 742, L30
- [12] Giuliani, A., Tavani, M., Bulgarelli, A., et al. 2010, *Astron. Astrophys.*, 516, L11+
- [13] Green, D. A. 2009, *Bulletin of the Astronomical Society of India*, 37, 45
- [14] Hoffman I.M. *et al.*, 2005, *ApJ*, 627, 803-812
- [15] Nolan, P. L., Abdo, A. A., Ackermann, M., et al. 2012, *ApJL*, 199, 31
- [16] Seta, M., Hasegawa, T., Dame, T. M., et al. 1998, *The Astrophysical Journal*, 505, 286
- [17] Seta M. *et al.*, 2004, *AJ*, 127, 1098-1116
- [18] Tavani, M., Giuliani, A., Chen, A. W., et al. 2010, *ApJ Lett.*, 710, L151
- [19] Torres, D. F., Rodriguez Marrero, A. Y., & de Cea Del Pozo, E. 2008, *MNRAS*, 387, L59
- [20] Yoshiike, S., Fukuda, T., Sano, H., et al. 2013, *ApJ*, 768, 179